Stem Cell Research (2013) 10, 417–427

Available online at www.sciencedirect.com

SciVerse ScienceDirect

www.elsevier.com/locate/scr

METHODS AND REAGENTS

EZ spheres: A stable and expandable culture system for the generation of pre-rosette multipotent stem cells from human ESCs and iPSCs

Allison D. Ebert [a,*], Brandon C. Shelley [b,1], Amanda M. Hurley [b,1], Marco Onorati [c,1], Valentina Castiglioni [c,1], Teresa N. Patitucci [a], Soshana P. Svendsen [b], Virginia B. Mattis [b], Jered V. McGivern [a], Andrew J. Schwab [a], Dhruv Sareen [b], Ho Won Kim [b], Elena Cattaneo [c], Clive N. Svendsen [b,**]

[a] *Department of Cell Biology, Neurobiology, and Anatomy, Medical College of Wisconsin, 8701 Watertown Plank Rd, Milwaukee, WI 53226, USA*
[b] *Cedars-Sinai Regenerative Medicine Institute, Cedars-Sinai Medical Center, 8700 Beverly Blvd, Los Angeles, CA 90048, USA*
[c] *Department of Biosciences and Centre for Stem Cell Research, Università degli Studi di Milano, Via Viotti 3/5, 20133 Milano, Italy*

Received 29 August 2012; received in revised form 19 January 2013; accepted 28 January 2013
Available online 4 February 2013

Abstract We have developed a simple method to generate and expand multipotent, self-renewing pre-rosette neural stem cells from both human embryonic stem cells (hESCs) and human induced pluripotent stem cells (iPSCs) without utilizing embryoid body formation, manual selection techniques, or complex combinations of small molecules. Human ESC and iPSC colonies were lifted and placed in a neural stem cell medium containing high concentrations of EGF and FGF-2. Cell aggregates (termed EZ spheres) could be expanded for long periods using a chopping method that maintained cell–cell contact. Early passage EZ spheres rapidly down-regulated OCT4 and up-regulated SOX2 and nestin expression. They retained the potential to form neural rosettes and consistently differentiated into a range of central and peripheral neural lineages. Thus, they

Abbreviations: AP2, activating protein 2; BLBP, brain lipid binding protein; BMP, bone morphogenetic proteins; CNS, central nervous system; DA, dopamine; DACH1, dachshund homolog 1; EB, embryoid body; EGF, epidermal growth factor; ESCs, embryonic stem cells; FGF-2, fibroblast growth factor; FOXG1, forkhead box protein G1; GBX2, gastrulation brain homeobox 2; HB9, homeobox gene Hb9; hESCs, human embryonic stem cells; HNK, human natural killer-1; HOXB4, homeobox B4; iPSCs, induced pluripotent stem cells; MAP2, microtubule-associated protein 2; MEF, mouse embryonic fibroblast; NG2, chondroitin sulphate proteoglycan; OCT4, octamer-binding transcription factor 4; OLIG2, oligodendrocyte transcription factor 2; OTX2, orthodenticle homeobox 2; PAR3, polarity complex gene 3; PAX6, paired box gene 6; PAX7, paired box gene 7; PCR, polymerase chain reaction; PDGFRα, platelet-derived growth factor alpha; PLZF, promyelocytic leukemia zinc finger; PNS, peripheral nervous system; SMAD, Sma and Mad related family; SOX1, SRY-related HMG-box 1; SOX2, SRY-related HMG-box 2; SSEA3, stage specific embryonic antigen 3; TGFβ, transforming growth factor beta; TH, tyrosine hydroxylase; Tuj1, βIII-tubulin; ZO-1, zona occludens protein 1

* Corresponding author. Fax: +1 414 955 6517.
** Corresponding author. Fax: +1 310 248 8066.
E-mail addresses: aebert@mcw.edu (A.D. Ebert), clive.svendsen@cshs.org (C.N. Svendsen).
[1] These authors contributed equally to this work.

1873-5061/$ - see front matter
http://dx.doi.org/10.1016/j.scr.2013.01.009

represent a very early neural stem cell with greater differentiation flexibility than other previously described methods. As such, they will be useful for the rapidly expanding field of neurological development and disease modeling, high-content screening, and regenerative therapies based on pluripotent stem cell technology.

Introduction

Human embryonic stem cells (hESCs) and induced pluripotent stem cells (iPSCs) have provided a platform for studying basic human development and disease mechanisms and hold great potential for future cell therapies (Murry and Keller, 2008). However, biomedical application of hESCs and iPSCs depends on the availability of robust cell expansion and differentiation protocols. Undifferentiated colonies of hESCs and iPSCs can be technically challenging to maintain and expand. For example, they thaw from frozen samples with low efficiency and then require co-culture with mouse embryonic fibroblasts (MEF), or expensive media and matrix proteins, in order to remain undifferentiated. Furthermore, they need daily medium changes, examination, and manual selection to ensure the cultures remain in an undifferentiated state. Finally, >10% of hESC and iPSC cultures develop karyotypic anomalies (Ben-David et al., 2011; Peterson et al., 2011; Taapken et al., 2011), which should be monitored as they could impact differentiation capabilities (Graf and Stadtfeld, 2008) and clinical applicability. Clearly, less time consuming and labor intensive culturing techniques would be advantageous.

Research into embryogenesis and nervous system development has been instrumental to the identification of factors required for cell specification. Using information gleaned from these studies, many groups have developed induction protocols to instruct hESCs and iPSCs to become a variety of neural cell types (Zhang et al., 2001), including motor neurons, dopamine neurons, striatal neurons, and oligodendrocytes (Aubry et al., 2008; Delli Carri et al., 2013; Li et al., 2005; Nistor et al., 2005; Perrier et al., 2004). Some of these traditional differentiation protocols use embryoid body (EB) formation as the first step of lineage restriction to mimic early human embryogenesis (Zhang et al., 2001), which is then followed by manual selection of neuroepithelial precursors. Interestingly, the efficiency of EB formation and subsequent differentiation can vary among hESC and iPSC lines, and in some instances fail using the same culturing conditions (Boulting et al., 2011; Hu et al., 2010; Osafune et al., 2008). While the mechanisms underlying these differences remain to be determined, this observation suggests that progressing through an EB step may not always be optimal. Additionally, EBs cannot be robustly expanded, so one must start with a large number of undifferentiated hESCs or iPSCs to generate enough EBs to push through the various differentiation steps for each experimental or therapeutic use, therefore increasing batch-to-batch variations among differentiation procedures.

A technique that efficiently expands neural stem cells from hESCs or iPSCs and allows consistent differentiation of neural tissue is of great interest, and there are a number of published protocols that have been developed (Chaddah et al., 2012; Elkabetz et al., 2008; Koch et al., 2009; Nemati et al., 2011). Elkabetz et al. (2008) used an extended EB formation period and sorting methods to isolate rosette stage neuroepithelial cells that allowed them to generate a transient population of expandable neural stem cells that retain differentiation potential. In contrast to other reports (Falk et al., 2012; Koch et al., 2009), only when these cells were grown in the presence of signaling molecules (e.g. sonic hedgehog and notch) were they able to retain rosette formation and structure, induce proliferation, and subsequently differentiate into motor neurons, dopamine neurons, and neural crest progenitor cells (Elkabetz et al., 2008). However, further expansion in the presence of growth factors resulted in the loss of rosette formation and in vitro regionalization capacity and biased the culture toward gliogenic differentiation (Elkabetz et al., 2008). Also, Koch et al. (2009) described a protocol in which neuroepithelial stem cells were mechanically isolated following EB formation and expanded in the presence of EGF and FGF-2 to successfully generate a variety of neural subtypes. However, cells became regionally restricted after ~15 in vitro passages (Falk et al., 2012; Koch et al., 2009).

In the current study we have devised a method that generates pre-rosette stem cells directly from hESCs and iPSCs in a free-floating aggregate system in the presence of EGF and FGF-2. Due to their ease of expansion and differentiation, we have termed these cultures "EZ spheres". Using our previously described method of a mechanical, non-enzymatic chopping technique (Svendsen et al., 1998), EZ spheres can be expanded for at least 30 passages while maintaining chromosomal stability. Given the proper neural differentiation conditions, rosettes appear within whole spheres and upon plate-down indicating that EZ spheres retain rosette properties after long-term exposure to EGF and FGF-2. Longitudinal analysis of neural gene expression patterns in EGF and FGF-2 culture conditions showed consistent and sustained expression of nestin and SOX2 for all lines, with more varied expression of region specific markers including FOXG1, GBX2, PAX7, and OTX2. Nevertheless, EZ spheres could be taken at any passage and placed into appropriate differentiation conditions to generate specialized neuronal and glial subtypes, such as dopamine neurons, motor neurons, striatal neurons, peripheral sensory neurons, astrocytes, and oligodendrocytes, with similar efficiencies between hESCs and iPSCs. Importantly, EZ spheres do not acquire regionally restricted differentiation potential over successive passages. As a result, the EZ sphere method eliminates the need for EB formation and manual selection, allows for exponential expansion of pre-rosette multipotent neural stem cells, is amenable to healthy and disease-specific iPSCs, and increases versatility of lineage specification over other published techniques.

Materials and methods

Cell culture

hESCs (H9 WiCell Research Institute) and iPSCs were grown on irradiated MEF as previously described (Thomson et al.,

1998). Human iPSCs were generated from fibroblast samples (4.2 line, GM003814 Coriell Institute; 21.8 line, GM002183 Coriell) using previously published protocols (Yu et al., 2007).

EZ sphere generation and passaging

EZ spheres were generated by lifting intact colonies from MEF feeder layers following collagenase treatment (1 mg/ml, Gibco) and placing them directly into a human neural progenitor growth medium (Stemline, Sigma) supplemented with 100 ng/ml basic fibroblast growth factor (FGF-2, Chemicon), 100 ng/ml epidermal growth factor (EGF, Chemicon), and 5 μg/ml heparin (Sigma) in ultra-low attachment flasks and were passaged weekly using a chopping technique (Svendsen et al., 1998).

Cryopreservation

The EZ spheres were settled into a pellet and transferred from EGF and FGF-2 supplemented media into serum-free, 8.7% DMSO-supplemented cell freezing media (Sigma). The cryovials were transported to a −80 °C freezer using an isopropyl alcohol chamber for 24 h. The frozen vials were then preserved for long-term in standard liquid nitrogen storage containers.

Karyotyping

EZ spheres were dissociated using TrypLE (Life Technologies), plated onto matrigel-coated, tissue culture treated T25 flasks in EGF and FGF-2 supplemented media, and grown to confluency. Standard G-banding chromosome analysis was performed by Cell Line Genetics (Madison, WI).

Cell counts

Prior to passaging, a small number of EZ spheres were dissociated using TrypLE and counted using trypan blue exclusion with either a glass hemocytometer or the TC-10 Cell Counter (Bio-Rad, Hercules, CA). The projected total cell number was calculated for each passage based on expansion data (Fig. 1C).

Differentiation

To induce astrocyte differentiation, spheres were dissociated with accutase (Chemicon) or TrypLE and plated onto poly-ornithine/laminin (Sigma) coated coverslips in Stemline with 2% B27 without growth factors for 2–4 weeks. Terminal differentiation into dopamine neurons, motor neurons, striatal neurons, sensory neurons, and oligodendrocytes followed previously published reports (Aubry et al., 2008; Lee et al., 2010; Li et al., 2005; Nistor et al., 2005; Schneider et al., 2007; Zhang et al., 2001). Briefly, spheres were removed from Stemline/EGF/FGF-2/heparin medium and placed in the appropriate induction media for terminal differentiation. At appropriate times, spheres were then plated onto poly-ornithine/laminin coated coverslips in growth factor supplemented media to achieve terminal differentiation and mature cell types (Fig. S3).

RNA isolation and PCR analysis

Total RNA was isolated using the RNeasy Mini Kit (Qiagen) with on-column DNase I digestion or Tri-Reagent (Sigma). cDNA was generated from 1 to 4 μg total RNA using SuperScript III (Invitrogen). RT-PCR and/or qRT-PCR were performed using specific primer sequences under standard conditions (Table S3).

Immunocytochemistry

Plated cells and whole spheres were fixed in 4% paraformaldehyde for 20 min at room temperature and rinsed with PBS. Spheres were sectioned at 15 μm using a cryostat and mounted onto microscope slides. Nonspecific labeling was blocked and the cells were permeabilized with 5% normal goat serum and/or 5% normal donkey serum and 0.2% Triton X-100 in PBS for 30 min at room temperature. Cells were rinsed with PBS and then incubated with primary antibodies (Table S4) for 1 h at room temperature or overnight at 4 °C. Cells were then labeled with the appropriate fluorescently-tagged secondary antibodies. Hoechst nuclear dye was used to label nuclei.

Imaging and cell counting analysis

Ten images were taken on at least three different fluorescently labeled coverslips per condition on a Leica DM6000B (Wetzlar, Germany) upright microscope using the LAS Advanced Fluorescence imaging software (version 2.4.1, Leica, Wetzlar, Germany). The images were then counted for antigen and Hoechst nuclear dye specificity using MetaMorph Software (Molecular Devices Inc., Sunnyvale, CA). The counts for each passage of each cell line were averaged as a single data point and then the three cell lines were plotted at each passage ($n = 3$). The data were statistically analyzed via a one-way ANOVA using a Bonferroni post-hoc test with Prism software (GraphPad, La Jolla, CA).

Electrophysiology

Whole cell voltage clamp and current clamp recordings were performed as described previously using an EPC 9 amplifier (HEKA, Germany) and Pulse software (version 8.78, HEKA, Lambrecht, Germany) (Dirajlal et al., 2003). Recording pipettes were pulled from fire-polished borosilicate capillary tubes (Sutter Instruments, Novato, CA) using a Flaming-Brown micropipette puller (Model P97, Sutter Instruments, Novato, CA). Pipette resistances ranged from 3 to 7 MΩ. Electrodes were back-filled with an intracellular buffer consisting of (in mM): KCl, 135; HEPES, 10; EGTA, 2; $MgCl_2$, 4.1; ATP, 2.5; GTP, 0.2; pH 7.2 (titrated with KOH); osmolality = 290 ± 3 mosM (adjusted with sucrose). Extracellular buffer consisted of (in mM): NaCl, 140; KCl, 5; $CaCl_2$, 2; $MgCl_2$, 1; HEPES, 10; glucose, 10; pH 7.4 (titrated with NaOH); osmolality = 310 ± 3 mosM. Putative astrocytes were targeted and identified based on morphology and lack of action potential generation. Current–voltage relationships were examined in voltage clamp mode by holding the cell membrane at a resting potential of −70 mV and then sequentially clamping the cell membrane for 100 ms at potentials ranging from −160 mV to +20 mV in 10 mV steps.

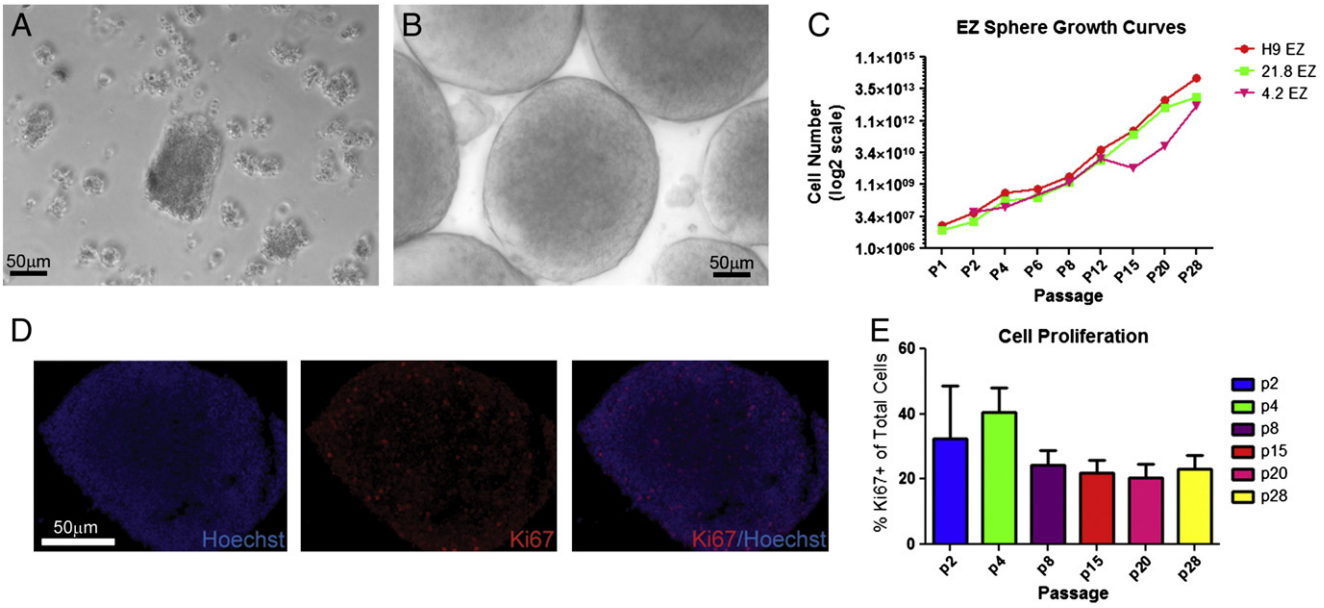

Figure 1 EZ spheres show stable growth over time. (A) Human 21.8 iPSC derived embryoid bodies displayed a fragmented and unhealthy appearance compared to (B) EZ spheres, which exhibited round, tightly packed aggregates. (C) All three EZ sphere lines showed similar expansion rates. The dip in expansion for 4.2 iPSC EZ spheres at passage 15 is attributed to changes in the growth medium lot, but they quickly recovered and were not significantly different by passage 28. (D) Cryosectioned 4.2 iPSC EZ spheres contain Ki67 positive proliferating cells. (E) Quantification of Ki67 immunofluorescent cells from all three EZ sphere lines shows consistent proliferation over time.

Results

There are a number of complex methods for the generation of neural subtypes from hESCs and iPSCs. In most of them, intact pluripotent colonies are first lifted, induced to form EBs, and then grown in the presence of lineage specific morphogens and growth factors to produce a variety of terminally differentiated neurons (dopamine, cholinergic, etc.), astrocytes, and oligodendrocytes (Murry and Keller, 2008). Although successful, this technique was not efficient for all iPSCs. For example, although all iPSCs generated EBs, over 50% of the EBs derived from both healthy and diseased iPSCs displayed an unhealthy appearance, such as tattered edges, fragmented and irregular shapes, membrane blebbing, and dark coloring, and did not efficiently survive neural specification (Fig. 1A). We therefore developed EZ spheres as an alternative to EB formation to consistently transition iPSCs from undifferentiated colonies to differentiated neural subtypes. Furthermore, in order to avoid potential bias in long-term differentiation potential, as shown in previously published protocols (Elkabetz et al., 2008; Koch et al., 2009; Nemati et al., 2011), we aimed to generate an expandable pre-rosette population of neural stem cells that could retain greater plasticity upon differentiation.

EZ spheres were generated by gently lifting the undifferentiated colonies from MEFs or Matrigel using enzymatic dissociation (e.g. collagenase, dispase), techniques consistent with EB generation protocols. Clumps of cells were then placed in ultra-low attachment flasks in neural progenitor cell medium consisting of 100 ng/ml EGF, 100 ng/ml FGF-2 (human or zebrafish), and 5 μg/ml heparin; the high level of EGF has previously been shown to increase the proliferation and neuronal potential of human fetal neural progenitor cells (Nelson et al., 2008). In this medium, the cells clustered into tightly compacted spheres with regular edges and a golden color within 3–5 days (Fig. 1B). EZ spheres continued to expand (many cultured for over a year), were passaged weekly by mechanical chopping, and could be cryopreserved and subsequently thawed with high efficiency. Cells within EZ spheres doubled in number every 7 days with approximately 20% of cells undergoing active proliferation at any one time based on Ki67 labeling (Figs. 1C–E). They also showed chromosomal stability for at least 30 passages (latest passage assessed) (Fig. S1).

We have produced and expanded EZ spheres from 19 independent hESC and iPSC lines, including healthy and disease-specific lines generated through multiple reprogramming methods, all of which demonstrates the robustness of the method (Table S1). In order to better characterize the composition and stability of EZ spheres, we undertook a systematic and longitudinal assessment using EZ spheres derived from H9 hESCs (Thomson et al., 1998) and two independent unaffected iPSC lines (Coriell fibroblast line GM003814 (4.2 iPSC), Coriell fibroblast line GM002183 (21.8 iPSC)). These iPSC lines have each been previously characterized for full reprogramming and down-regulation of exogenous transgene expression (Ebert et al., 2009; HD iPSC Consortium, 2012). First, EZ spheres were analyzed for various pluripotency and neural progenitor markers at 0, 2, 4, 8, 15, 20, and 28 passages post-sphere formation by immunocytochemistry. Specifically, we found that nearly 75% of cells derived from all three stem cell lines were

positive for OCT4 (endogenous *POU5F1*) immediately following sphere formation (passage 0), but this dramatically decreased by passage 2 and was virtually absent in subsequent passages (Fig. 2A). Further, immunocytochemical analysis of dissociated EZ spheres showed that there was a significant increase in nestin expression after passage 2, such that >60% of cells were nestin positive after passage 4 and >90% of cells by passage 7 (Fig. 2B). Next, immunocytochemistry of intact EZ spheres showed expression of neural progenitor and radial glial markers such as nestin, PAX6, vimentin, BLBP, SOX1, and SOX2 throughout the spheres, but limited expression of the motor neuron and/or oligodendrocyte progenitor marker OLIG2, the mature neuronal marker MAP2, or pluripotency markers Nanog, SSEA3, and Tra-1-81 (Fig. 2C).

As a first step to assess the cellular composition in EZ spheres, we performed PCR analysis for a variety of pluripotent and region specific markers (Fig. 3A). At passage 12, 21.8 iPSC-derived EZ spheres showed expression of a number of early neural progenitor (nestin, SOX1, Dach1) and posterior markers (HOXB4, GBX2), but limited expression of more anterior markers (FOXG1, OTX2) suggesting EZ spheres may also undergo regional specification during extended culturing as has been shown by others (Elkabetz et al., 2008; Koch et al., 2009). To more thoroughly assess this question, we examined gene expression by PCR at every passage out to 32 using a set of regional identity markers: neural ectoderm (SOX2, nestin, PAX6), anterior (FOXG1, OTX2), posterior (GBX2), dorsal (PAX7), neural crest (HNK1), and undifferentiated stem cells (OCT4). Representative PCR gels for undifferentiated colonies and EZ spheres at passages 0, 9, 18, and 27 (Fig. 3B) show basal expression levels among the lines and passages (a compiled table indicating relative expression at all passages is presented in Table S2). OCT4 expression was detected only in early passages and was silenced in all lines consistent with the immunocytochemistry results (Figs. 2A, 3B). Nestin, SOX2, and HNK1 were consistently expressed in all three lines through late passages, indicating maintenance of a neural progenitor cell population amenable to both central and peripheral nervous system subtypes (Fig. 3B, Table S2). Nestin was detected in undifferentiated colonies in all lines, which is consistent with previously reported data (Keil et al., 2012). PCR analysis for region specific markers showed fluctuations in gene expression levels over successive passages while maintained in EGF/FGF-2 growth conditions. For example, OTX2 was expressed at high levels in nearly every passage of H9 hESC- and 4.2 iPSC-derived EZ spheres, but not in 21.8 iPSC-derived EZ spheres (Fig. 3B, Table S2). On the other hand, PAX6, PAX7, FOXG1, and GBX2 were detected only sporadically at early and late passages in all lines (Fig. 3B, Table S2). Taken together, these data highlight that EZ spheres maintained long-term in EGF and FGF-2 are dynamic across passages, but that there is not a selective growth advantage for one regional progenitor cell over another. Additionally, gene expression patterns appear to be influenced by inherent properties of each cell line, similar to previously reported results (Boulting et al., 2011), rather than the culture conditions.

Columnar neuroepithelial-like cells identified within rosette structures are a hallmark of neural progenitor cells and are found transiently in EBs or monolayer differentiation protocols during lineage restriction of hESCs toward neural subtypes (Chambers et al., 2009; Zhang et al., 2001). We therefore tested whether cells in EZ spheres were representative of a pre-rosette neural stem cell population that could be extensively expanded. We examined rosette markers by immunocytochemistry using intact spheres at multiple EZ sphere passages (13, 16, 21, and 28). Sections through 21.8 iPSC EZ spheres grown in EGF and FGF-2 did not reveal immunolabeling for PLZF, ZO-1, or N-cadherin (Figs. 4A, B), which are all standard markers used to identify the apical orientation of rosettes (Abranches et al., 2009). However, following 7 days of neural induction initiated by removing EGF and FGF-2 and supplementing with N2 and BDNF, rosettes characterized by a central lumen and radially disposed neuroepithelial cells appeared and robustly expressed PLZF in conjunction with apical rosette markers ZO-1, PAR3, β-catenin, and N-cadherin (Figs. 4C–J). Importantly, rosettes were also detected in whole sections through 4.2 iPSC EZ spheres as well as upon plate-down of H9 hESC EZ spheres following 1 week of neural differentiation (Fig. S2). These data indicate that neural stem cells within EZ spheres are captured in a self-renewing, pre-rosette stage, which precedes the long-term neural stem cell (LT-hESNSC) stage described by Koch and colleagues (Koch et al., 2009).

We next aimed to test the differentiation capabilities of the EZ spheres. We found that at any passage for all cell lines regardless of cryopreservation, EZ spheres can be placed in specific neural induction media for terminal neuronal or glial cell differentiation using protocols adapted from those reported previously (Aubry et al., 2008; Lee et al., 2010; Li et al., 2005; Nistor et al., 2005; Schneider et al., 2007; Zhang et al., 2001) (Fig. S3). Methods in which EB formation is the initial step in differentiation, EZ spheres were substituted for EBs. Using the EZ sphere technique for both hESCs and iPSCs, we show the generation of various neuronal cells (Fig. 5A), including dopamine neurons (Fig. 5B), motor neurons (Fig. 5C), striatal neurons (Fig. 5D), neural crest progenitor cells (Fig. 5E), and peripheral sensory neurons (Fig. 5F).Using glial differentiation protocols (Fig. 5G), we were able to generate oligodendrocytes and astrocytes from EZ spheres. Importantly, we have previously shown that neurons derived from EZ spheres are electrophysiologically active (HD iPSC Consortium, 2012). Similarly, EZ sphere derived astrocytes express typical potassium channel properties (Fig. S4). Differentiations presented in Fig. 5 are from passages ranging from 5 to 36 with no variation in differentiation efficiency (data not shown). Previous studies have demonstrated increased neural differentiation following inhibition of TGFβ, activin, and BMP (Chambers et al., 2009). We therefore tested whether this dual SMAD inhibition would increase nestin expression in p3 H9 hESC EZ spheres. However, we found no difference in nestin expression between treated and untreated EZ spheres using both immunocytochemistry and PCR (Fig. S5).

Finally, we wanted to directly compare the differentiation efficiency between the traditional EB method and the EZ sphere method. Using H9 hESCs, we performed simultaneous directed differentiation toward tyrosine hydroxylase (TH) positive neurons by exposing EB and EZ spheres to FGF-8 and sonic hedgehog as described previously (Schneider et al., 2007). Importantly, EZ spheres do not generate TH dopamine neurons when cultured only in the presence of EGF and FGF-2 (Fig. 6B). However, treatment of floating EZ spheres with FGF-8 for two weeks, FGF-8 and sonic hedgehog for one week, and maturation of plated cells in

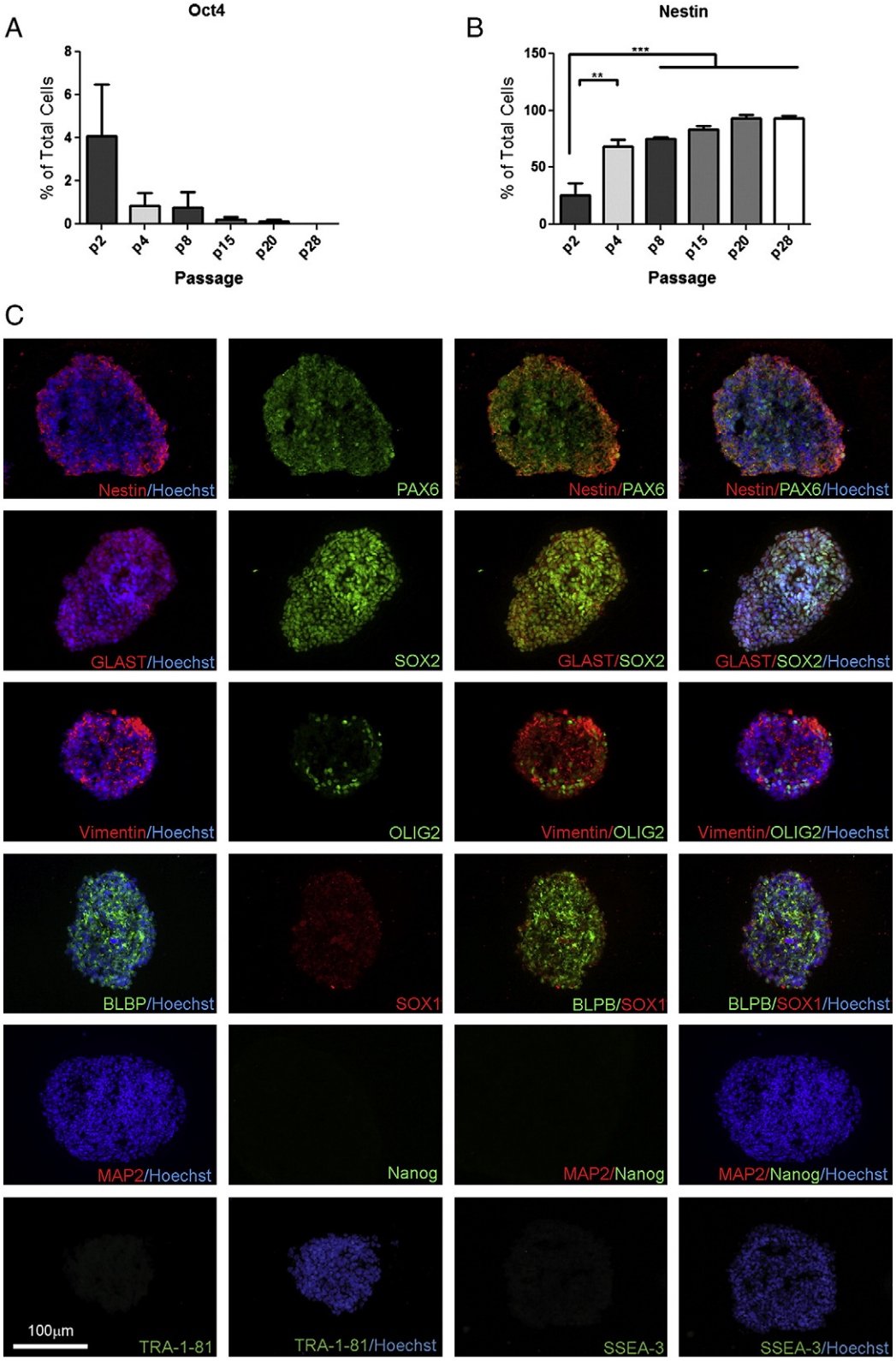

Figure 2 EZ spheres rapidly up-regulate neural progenitor markers. (A) Combined data from dissociated cells from the three EZ sphere lines showed nearly immediate decline in the pluripotency marker OCT4 and (B) a corresponding increase in the neural progenitor marker nestin. (C) Immunocytochemistry for a variety of pluripotency and lineage markers was performed on cryosectioned whole 21.8 iPSC EZ spheres at passage 13. The pluripotency markers TRA-1-81, Nanog, and SSEA-3 were absent in the spheres, whereas neural progenitor markers nestin, PAX6, SOX2, and SOX1 were readily expressed. Additional radial glial markers vimentin and BLBP and the glutamate transporter GLAST were highly expressed in EZ spheres, although the motor neuron/oligodendrocytes progenitor marker OLIG2 and the mature neuron marker MAP2 were nearly absent. **$p<0.001$; ***$p<0.0001$.

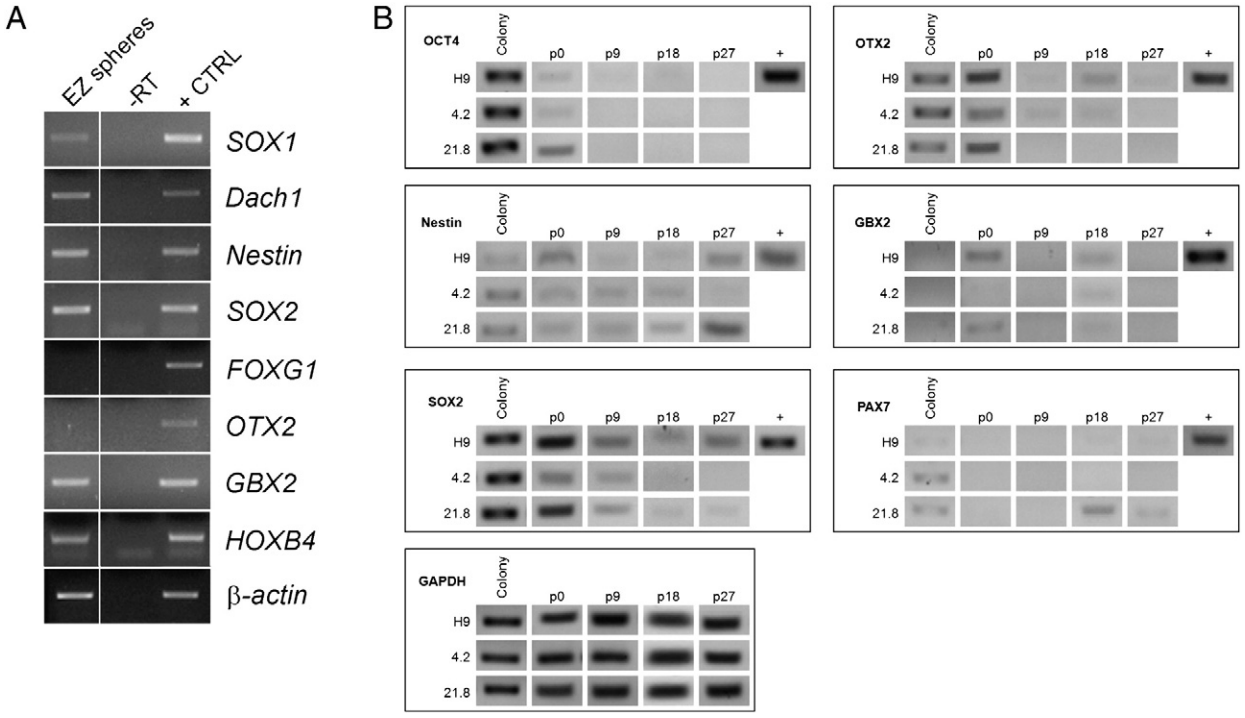

Figure 3 Longitudinal gene expression highlights dynamic properties of EZ spheres. (A) Passage 13 EZ spheres from 21.8 iPSCs showed high expression of neural progenitor markers and posterior markers, but no expression of anterior forebrain markers. Actin was used for a control. (B) Longitudinal PCR analysis for regional markers across multiple passages showed both up-regulated and down-regulated expression of region-specific genes over time. GAPDH was used as a control.

growth factor supplemented medium (Fig. S3) generated TH/Tuj1 double positive neurons in equal numbers to those generated using the EB dopamine neuron differentiation method (Figs. 6A, B). In all the differentiations we have attempted thus far using EZ spheres, efficiencies are comparable to standard EB differentiation protocols reported in the literature, they proceed through a similar time line as neural cells derived using traditional EB methods, and display up-regulation of appropriate transcription factors and markers as would be indicative of regional specification for a particular neural cell type. For example, the ventral hindbrain/spinal cord markers ISLET1 and HB9 were detected in EZ sphere cultures undergoing motor neuron differentiation (Fig. 5C). Similarly, prior to the generation of peripherin positive sensory neurons, neural crest markers AP2 and p75 were significantly up-regulated indicating the appropriate lineage restriction process is followed (Fig. 5E). The anterior forebrain markers OTX2 and FOXG1 were highly expressed as early as 7 days following transition into the striatal differentiation conditions using 21.8 iPSC EZ spheres (Fig. S6). This is particularly important because 21.8 iPSC EZ spheres did not show expression of OTX2 and FOXG1 while expanded in EGF and FGF-2 (Fig. 3B, Table S2). Finally, during glial differentiation we detected increased expression of progenitor and more mature markers including NG2, PDGFRα, S100, and ALDH1L1 (data not shown). Taken together, these data highlight that EZ spheres expanded in EGF and FGF-2 maintain multipotent neural stem cells responsive to multiple regional cues that generate differentiated cell types in equivalent efficiencies to more complex methods.

Discussion

Generating neural stem cells from hESCs and iPSCs has been successfully achieved by a number of groups (Elkabetz et al., 2008; Falk et al., 2012; Koch et al., 2009; Nemati et al., 2011). However, the simplicity and retained – or even enhanced – differentiation versatility combined with economical aspects of their growth (e.g. minimal medium components and reduced hands-on maintenance) are distinct advantages of the EZ sphere method over other published protocols. EZ spheres also recover from cryostorage with high efficiency, thus facilitating experimental use.

EZ spheres do not require EB formation or manual selection processes, yet they still can be efficiently patterned into a variety of neural subtypes without acquiring regional differentiation bias over time, an advantage over other published protocols (Falk et al., 2012; Koch et al., 2009; Nemati et al., 2011). Moreover, properly organized rosette structures can be generated even after long-term culture in EGF and FGF-2. Because EZ spheres are captured prior to rosette formation, they do not show rosette markers without neural induction (Fig. 4). This suggests that EZ spheres expand the earliest neural stem cell population so far identified, which can be positioned at a pre-rosette stage and before LT-hESNSCs (Koch et al., 2009), therefore bearing greater flexibility in terms of terminal differentiation. Although selecting preformed rosettes increases the purity of the differentiated neural cultures, this may also be limiting their differentiation potential as previous work has shown that hESC-derived neural progenitor cells are restricted by the time SOX1 is

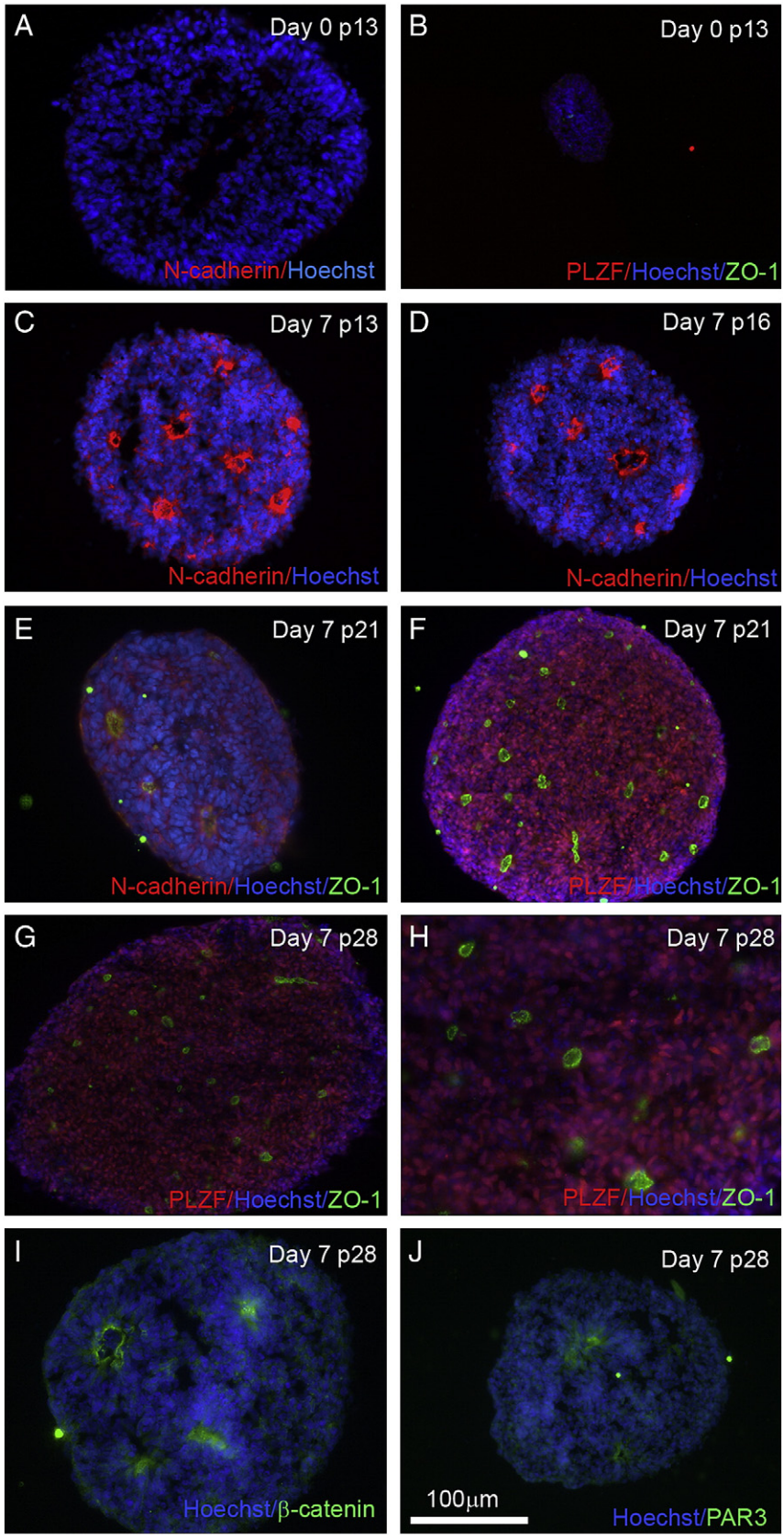

Figure 4 EZ spheres can generate well-formed rosettes. (A, B) Immunocytochemistry of whole cryosectioned 21.8 iPSC EZ spheres showed no rosette formation in the absence of neural induction. In contrast, after 7 days of neural induction EZ spheres exhibited expression of the rosette markers (C–E) N-cadherin, (E–H) ZO-1, (F–H) PLZF, (I) β-catenin, and (J) PAR3. Passage number and marker used are indicated.

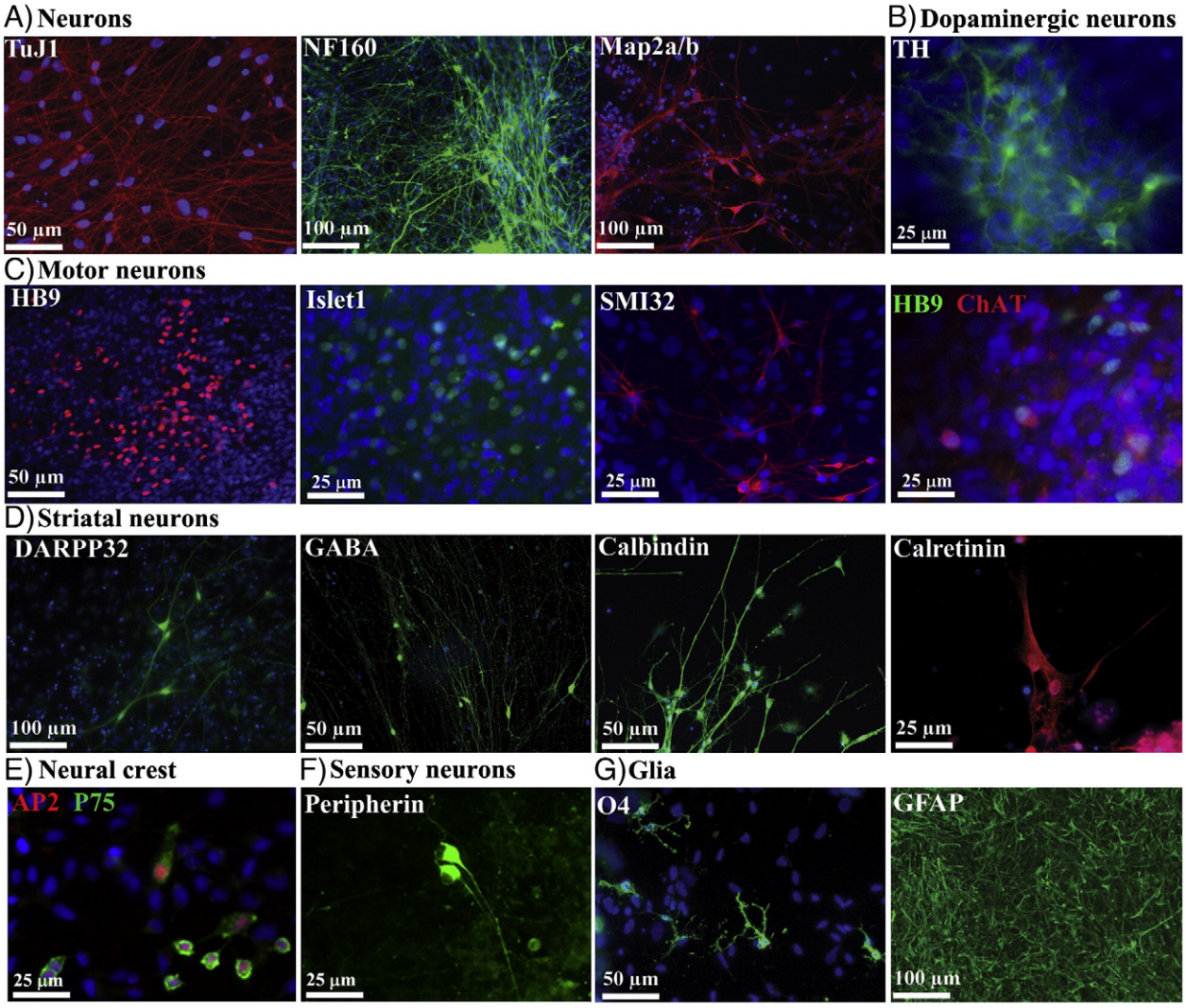

Figure 5 Upon directed differentiation, EZ spheres readily produce cells within the neural lineage. Immunocytochemical staining of various lineage markers showed that EZ spheres could generate (A) TuJ1, NF160, and MAP2a/b positive neurons, (B) TH positive dopamine neurons, (C) HB9, ISLET1, SMI32R, and ChAT positive motor neurons, (D) DARPP32, GABA, calbindin and calretinin positive striatal neurons, (E) AP2 and p75 positive neural crest progenitor cells, and (F) peripherin positive sensory neurons. (G) EZ spheres could also generate cells of glial lineage, including O4 positive immature oligodendrocytes and GFAP positive astrocytes. Nuclei are labeled with Hoechst in blue. A and D are from 21.8 iPSC EZ spheres; B, E, and F are from H9 hESC EZ spheres; C and G are from 4.2 iPSC EZ spheres.

expressed in well formed rosettes (Li et al., 2005). It may also be possible that retaining non-neurally committed cell types in the spheres exposes the cells to signaling processes more consistent with in vivo development including early instruction from mesoderm (Lumsden and Krumlauf, 1996). EZ spheres express the mesodermal marker Brachyury as well as the endodermal marker alpha fetoprotein (data not shown), which may be contributing to the diverse differentiation potential. However, EZ spheres are not simply fully undifferentiated stem cells grown in suspension culture similar to those described by Steiner et al. (2010). OCT4, Nanog, SSEA3, and Tra-1-81 expression were significantly down-regulated in EZ spheres almost immediately after sphere formation (Fig. 2) indicating that EGF and FGF-2 in combination are not capable of maintaining a large population of undifferentiated stem cells in suspension.

Our longitudinal examination of neural gene expression by PCR showed that EGF and FGF-2 maintain a heterogeneous population of cells within the spheres. Although central and peripheral neural progenitor genes nestin, SOX2, and HNK1 were consistently expressed, other region specific markers were differentially expressed over time. Because of this heterogeneity, it is possible that the signal for lowly expressing genes was below our level of detection. However, we interpret this dynamic nature of gene expression within EZ spheres as a contributing factor toward their diverse differentiation potential, likely by allowing cells to effectively respond to external differentiation cues even at later passages. As such, when EZ spheres are removed from EGF and FGF-2 and placed into appropriate differentiation media, the cells retain the capacity to up-regulate appropriate regionalization genes and consistently produce specified neurons and

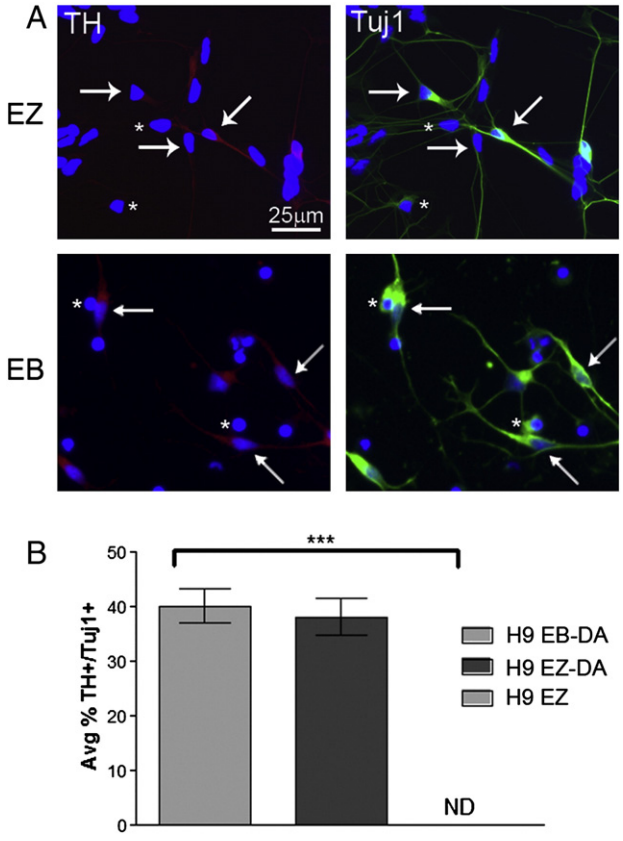

Figure 6 Dopamine (DA) neuron differentiation efficiency is comparable between EZ spheres and EBs. (A) Following treatment with FGF-8 and sonic hedgehog, H9 EZ spheres and H9 EBs generated TH+ cells (red) that co-labeled with the neuronal marker Tuj1 (green). Arrows indicate TH+/Tuj1+ cells; asterisks indicate TH−/Tuj1+ cells. (B) Four weeks after directed differentiation in the presence of FGF-8 and sonic hedgehog signaling, there was no significant difference in the number of TH+/Tuj1+ neurons generated in H9 hESC EBs (EB-DA) and H9 hESC EZ spheres (EZ-DA). H9 hESC EZ spheres do not generate TH positive neurons in the absence of FGF-8 and sonic hedgehog signaling (EZ; ND=not detected). ***$p<0.0001$.

glia. Furthermore, terminal differentiation from EZ spheres shows similar efficiencies compared to standard EB protocols. Efficient neural differentiation has been described by using dual SMAD inhibition during hESC and iPSC patterning (Chambers et al., 2009). Importantly, EZ spheres are easily adaptable to this step as inhibitors to TGFβ, activin, and BMP (e.g. noggin and SB431542) can be added directly to floating EZ spheres at the start of the directed differentiation, as was done for the sensory neuron differentiation (Fig. S3). Although dual SMAD inhibition did not increase nestin expression in early passage H9 hESC-derived EZ spheres (Fig. S5), further optimization and increased yield of terminally differentiated neural subtypes may be achieved by incorporating this in the EZ sphere differentiation protocols.

In summary, this simple protocol allows rapid expansion of early multipotent stem cells that carry a pre-rosette identity and retain the potential to produce many cell types of CNS and PNS origin. Our established EZ sphere culture method may help facilitate the wide range of clinical science applications for hESC- and iPSC-derived neural tissue.

Supplementary data to this article can be found online at http://dx.doi.org/10.1016/j.scr.2013.01.009.

Author contributions

A.D.E. and C.N.S. developed the method to generate EZ spheres. A.D.E., B.C.S., V.B.M, J.V.M, A.J.S., and D.S. tested and adapted the differentiation protocols using hESC- and iPSC-derived EZ spheres and performed data analysis. A.M.H., T.N.P., and S.P.S. performed data analysis. H.W.K. conducted differentiation experiments, and M.O., V.C., and E.C. performed EZ sphere rosette characterization, differentiation, and analysis. A.D.E., C.N.S., and E.C. wrote the manuscript. All authors had final approval of the manuscript.

Acknowledgments

The authors thank B. Heins, A. Barber, and E. McMillan for technical assistance and A. Weyer for astrocyte electrophysiology. This work was supported by NIH/NINDS P01NS057778 (CNS), NIH/CHHD R21HD060899 (ADE), Advancing a Healthier Wisconsin (ADE), the ALS Association (CNS), and CHDI Foundation, New York (EC). TNP was supported by the Quadracci Memorial Fellowship.

References

Abranches, E., Silva, M., Pradier, L., Schulz, H., Hummel, O., Henrique, D., Bekman, E., 2009. Neural differentiation of embryonic stem cells in vitro: a road map to neurogenesis in the embryo. PLoS One 4, e6286.

Anderova, M., Antonova, T., Petrik, D., Neprasova, H., Chvatal, A., Sykova, E., 2004. Voltage-dependent potassium currents in hypertrophied rat astrocytes after a cortical stab wound. Glia 48, 311–326.

Aubry, L., Bugi, A., Lefort, N., Rousseau, F., Peschanski, M., Perrier, A.L., 2008. Striatal progenitors derived from human ES cells mature into DARPP32 neurons in vitro and in quinolinic acid-lesioned rats. Proc. Natl. Acad. Sci. U. S. A. 105, 16707–16712.

Ben-David, U., Mayshar, Y., Benvenisty, N., 2011. Large-scale analysis reveals acquisition of lineage-specific chromosomal aberrations in human adult stem cells. Cell Stem Cell 9, 97–102.

Boulting, G.L., Kiskinis, E., Croft, G.F., Amoroso, M.W., Oakley, D.H., Wainger, B.J., Williams, D.J., Kahler, D.J., Yamaki, M., Davidow, L., et al., 2011. A functionally characterized test set of human induced pluripotent stem cells. Nat. Biotechnol. 29, 279–286.

Chaddah, R., Arntfield, M., Runciman, S., Clarke, L., van der Kooy, D., 2012. Clonal neural stem cells from human embryonic stem cell colonies. J. Neurosci. 32, 7771–7781.

Chambers, S.M., Fasano, C.A., Papapetrou, E.P., Tomishima, M., Sadelain, M., Studer, L., 2009. Highly efficient neural conversion of human ES and iPS cells by dual inhibition of SMAD signaling. Nat. Biotechnol. 27, 275–280.

Delli Carri, A., Onorati, M., Lelos, M.J., Castiglioni, V., Faedo, A., Menon, R., Camnasio, S., Vuono, R., Spaiardi, P., Talpo, F., et al., 2013. Developmentally coordinated extrinsic signals drive human pluripotent stem cell differentiation toward authentic DARPP-32+ medium-sized spiny neurons. Development 140, 301–312.

Dirajlal, S., Pauers, L.E., Stucky, C.L., 2003. Differential response properties of IB(4)-positive and -negative unmyelinated sensory neurons to protons and capsaicin. J. Neurophysiol. 89, 513–524.

Ebert, A.D., Yu, J., Rose Jr., F.F., Mattis, V.B., Lorson, C.L., Thomson, J.A., Svendsen, C.N., 2009. Induced pluripotent stem cells from a spinal muscular atrophy patient. Nature 457, 277–280.

Elkabetz, Y., Panagiotakos, G., Al Shamy, G., Socci, N.D., Tabar, V., Studer, L., 2008. Human ES cell-derived neural rosettes reveal a functionally distinct early neural stem cell stage. Genes Dev. 22, 152–165.

Falk, A., Koch, P., Kesavan, J., Takashima, Y., Ladewig, J., Alexander, M., Wiskow, O., Tailor, J., Trotter, M., Pollard, S., et al., 2012. Capture of neuroepithelial-like stem cells from pluripotent stem cells provides a versatile system for in vitro production of human neurons. PLoS One 7, e29597.

Graf, T., Stadtfeld, M., 2008. Heterogeneity of embryonic and adult stem cells. Cell Stem Cell 3, 480–483.

HD iPSC Consortium, 2012. Induced pluripotent stem cells from patients with Huntington's disease show CAG repeat expansion-associated phenotypes. Cell Stem Cell 11, 264–278.

Hu, B.Y., Weick, J.P., Yu, J., Ma, L.X., Zhang, X.Q., Thomson, J.A., Zhang, S.C., 2010. Neural differentiation of human induced pluripotent stem cells follows developmental principles but with variable potency. Proc. Natl. Acad. Sci. U. S. A. 107, 4335–4340.

Keil, M., Siegert, A., Eckert, K., Gerlach, J., Haider, W., Fichtner, I., 2012. Transcriptional expression profile of cultured human embryonic stem cells in vitro and in vivo. In Vitro Cell. Dev. Anim. 48, 165–174.

Koch, P., Opitz, T., Steinbeck, J.A., Ladewig, J., Brustle, O., 2009. A rosette-type, self-renewing human ES cell-derived neural stem cell with potential for in vitro instruction and synaptic integration. Proc. Natl. Acad. Sci. U. S. A. 106, 3225–3230.

Lee, G., Chambers, S.M., Tomishima, M.J., Studer, L., 2010. Derivation of neural crest cells from human pluripotent stem cells. Nat. Protoc. 5, 688–701.

Li, X.J., Du, Z.W., Zarnowska, E.D., Pankratz, M., Hansen, L.O., Pearce, R.A., Zhang, S.C., 2005. Specification of motoneurons from human embryonic stem cells. Nat. Biotechnol. 23, 215–221.

Lumsden, A., Krumlauf, R., 1996. Patterning the vertebrate neuraxis. Science 274, 1109–1115.

Murry, C.E., Keller, G., 2008. Differentiation of embryonic stem cells to clinically relevant populations: lessons from embryonic development. Cell 132, 661–680.

Nelson, A.D., Suzuki, M., Svendsen, C.N., 2008. A high concentration of epidermal growth factor increases the growth and survival of neurogenic radial glial cells within human neurosphere cultures. Stem Cells 26, 348–355.

Nemati, S., Hatami, M., Kiani, S., Hemmesi, K., Gourabi, H., Masoudi, N., Alaei, S., Baharvand, H., 2011. Long-term self-renewable feeder-free human induced pluripotent stem cell-derived neural progenitors. Stem Cells Dev. 20, 503–514.

Nistor, G.I., Totoiu, M.O., Haque, N., Carpenter, M.K., Keirstead, H.S., 2005. Human embryonic stem cells differentiate into oligodendrocytes in high purity and myelinate after spinal cord transplantation. Glia 49, 385–396.

Osafune, K., Caron, L., Borowiak, M., Martinez, R.J., Fitz-Gerald, C.S., Sato, Y., Cowan, C.A., Chien, K.R., Melton, D.A., 2008. Marked differences in differentiation propensity among human embryonic stem cell lines. Nat. Biotechnol. 26, 313–315.

Perrier, A.L., Tabar, V., Barberi, T., Rubio, M.E., Bruses, J., Topf, N., Harrison, N.L., Studer, L., 2004. Derivation of midbrain dopamine neurons from human embryonic stem cells. Proc. Natl. Acad. Sci. U. S. A. 101, 12543–12548.

Peterson, S.E., Westra, J.W., Rehen, S.K., Young, H., Bushman, D.M., Paczkowski, C.M., Yung, Y.C., Lynch, C.L., Tran, H.T., Nickey, K.S., et al., 2011. Normal human pluripotent stem cell lines exhibit pervasive mosaic aneuploidy. PLoS One 6, e23018.

Schneider, B.L., Seehus, C.R., Capowski, E.E., Aebischer, P., Zhang, S.C., Svendsen, C.N., 2007. Over-expression of alpha-synuclein in human neural progenitors leads to specific changes in fate and differentiation. Hum. Mol. Genet. 16, 651–666.

Steiner, D., Khaner, H., Cohen, M., Even-Ram, S., Gil, Y., Itsykson, P., Turetsky, T., Idelson, M., Aizenman, E., Ram, R., et al., 2010. Derivation, propagation and controlled differentiation of human embryonic stem cells in suspension. Nat. Biotechnol. 28, 361–364.

Svendsen, C.N., ter Borg, M.G., Armstrong, R.J., Rosser, A.E., Chandran, S., Ostenfeld, T., Caldwell, M.A., 1998. A new method for the rapid and long term growth of human neural precursor cells. J. Neurosci. Methods 85, 141–152.

Taapken, S.M., Nisler, B.S., Newton, M.A., Sampsell-Barron, T.L., Leonhard, K.A., McIntire, E.M., Montgomery, K.D., 2011. Karotypic abnormalities in human induced pluripotent stem cells and embryonic stem cells. Nat. Biotechnol. 29, 313–314.

Thomson, J.A., Itskovitz-Eldor, J., Shapiro, S.S., Waknitz, M.A., Swiergiel, J.J., Marshall, V.S., Jones, J.M., 1998. Embryonic stem cell lines derived from human blastocysts. Science 282, 1145–1147.

Yu, J., Vodyanik, M.A., Smuga-Otto, K., Antosiewicz-Bourget, J., Frane, J.L., Tian, S., Nie, J., Jonsdottir, G.A., Ruotti, V., Stewart, R., et al., 2007. Induced pluripotent stem cell lines derived from human somatic cells. Science 318, 1917–1920.

Zhang, S.C., Wernig, M., Duncan, I.D., Brustle, O., Thomson, J.A., 2001. In vitro differentiation of transplantable neural precursors from human embryonic stem cells. Nat. Biotechnol. 19, 1129–1133.